NUMERICAL ANALYSIS OF DAMAGED CONCRETE MICROSTRUCTURES

D. C. Borges[12], J. J. C. Pituba.[1]

[1]*Federal University of Catalão*
St. Universitário, Catalão/Goiás, Brasil
dannilo.borges@ifg.edu.br, julio_pituba@ufcat.edu.br
[2]*Instituto Federal de Goiás*
R. São Bartolomeu, Vila Esperança, Luziânia/Goiás, Brasil
dannilo.borges@ifg.edu.br

Abstract. The numerical analysis of the mechanical behaviour of composite materials considering the specificity of each of its phases requires complex models leading sometimes to unfeasible analyses. Thus, the present work deals with the modelling of the mechanical behaviour of damaged heterogeneous materials within a multiscale approach in order to overcome this problem. The modelling is based on the concept of Representative Volume Element (RVE) representing the microstructure of the concrete, using the Finite Element Method (FEM) to perform a computational homogenization within the multiscale approach. The matrix is considered as a damaged material following the Mazars´ damage model. Linear elastic behaviour is adopted to aggregates. To represent the transition zone, contact and cohesive finite elements are considered. The main objective is to show that the damage material can be represented by a formulation based on a computational homogenization technique considering a multiscale approach. Results of representative microstructures of the concrete submitted to deformation states are presented and the homogenized responses obtained show the expected behaviour of the concrete.

Keywords: multi-scale modelling, homogenization, fracture model, damage model

1 Introduction

Concrete is a material widely used in building construction. It is a material that exhibits mechanical behaviour that is complex to be computationally modelled as stated by Pituba and Fernandes [1] and Voyiadjis et al. [2]. Several constitutive theories have emerged to determine the mechanical behaviour of concrete by observing the macroscopic properties. However, these theories do not consider the characteristics of each constituent material and its microstructure.

One way to avoid this problem is through Multiscale modelling. Several works already apply this modelling to simulate the behaviour of concrete as Giusti et al. [3], Fernandes et al. [4], Pituba et al [5], Wang et al. [6] and Congro et al. [7]. In Multiscale modelling it is possible to have an integration of the behaviour that happens on a smaller scale up to the macroscopic level, obtaining the behaviour response more precisely.

Within the various phenomena existing in concrete, dissipative phenomena coming from damage and fracturing process are the object of study in this work. In this context, the Continuum Damage Mechanics has been developed allowing the quantification of damage processes in the microstructure and it describes the influence of these effects on mechanical behaviour. Among the damage models, the Mazars model [8] is one of the simplest and it allows a good computational modelling.

Another phenomenon observed in concrete is the brittle behaviour in the transition zone, between the cement paste and aggregates. This transition zone is the most brittle region of the material. It is because of the presence of this transition zone that concrete rupture occurs at a lower stress level than the resistance of other constitutive phases (Mehta and Monteiro [9]). To model this region, a model developed by Pituba and Souza Neto [10] that used the concepts of Fracture Mechanics is used. In a heterogeneous material when cracking process in many cases is the dominant phenomenon on nonlinear behaviour, Fracture Mechanics is able to provide appropriate constitutive models (Borges et al [11]).

2 Concrete Model

To simulate the micromechanical behaviour of concrete, a formulation for a Representative Volume Element (RVE) has been proposed to represent the microstructure. A macroscopic strain vector is imposed on its macrostructure and thus the microscopic constitutive stresses and tensors can be calculated in the microstructure. Theories of homogenization and the average volume concepts between the macro and microscale are adopted with different values of stresses and homogenized tensors being obtained according to geometric distribution and proportionality between the materials. In addition, multiscale models have different boundary conditions imposed to the RVE. In this work only the microstructure is analysed in the context of multiscale analysis, but a fully coupled structure analysis was not presented.

To simulate the mechanical behaviour of concrete, the RVE discretization is given by the Finite Element Method with triangular elements. Aggregates are considered to be approximately circular and obey linear elastic behaviour. The cement paste presents the elastic behaviour with the Mazars Damage Model. In order to simulate the opening and/or closing of microcracks in the transition zone, contact and cohesive fracture elements are used as shown in Figure 1.

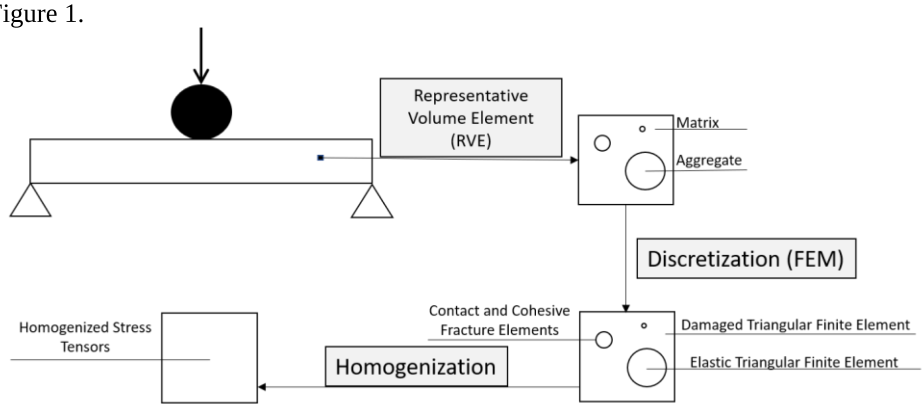

Figure 1. RVE Scheme

2.1 Multiscale model on the mesoscale

For this work, the RVE is described as continuous so that the concept of stress remains valid in mesoscale and RVE should be large enough for its continuum medium representation makes sense. The entire formulation described in this part has been based on Fernandes et al. [4]. Consider that the strain tensor ε (x,t) and the stress tensor σ (x, t) at a given point x of the macroscopic body is the average volume of its respective microscopic field $\varepsilon_\mu = \varepsilon_\mu$ (x,t) or $\sigma_\mu = \sigma_\mu$ (x,t) about the RVE associated with point x at an arbitrary time:

$$\varepsilon(x,t) = \frac{1}{V_\mu}\int_{\Omega_\mu} \varepsilon_\mu(y,t)dV \tag{1}$$

$$\sigma(x,t) = \frac{1}{V_\mu}\int_{\Omega_\mu} \sigma_\mu(y,t)dV \tag{2}$$

Since the field of microscopic strain is decomposed by the following sum:

$$\varepsilon_\mu(y,t) = \varepsilon(x,t) + \tilde{\varepsilon}_\mu(y,t) \tag{3}$$

Where ε is constant and represents the homogenized strain imposed on the RVE given by the macro-continuum and $\tilde{\varepsilon}_\mu$ is called floating deformation field. After some mathematical manipulations demonstrated by Fernandes et al. [4] it is possible to rewrite Equation (3) in velocity form, where a microscopic strain velocity is said to be kinematically admissible if:

$$\dot{\varepsilon}_\mu(y,t) = \nabla^S \dot{u}_\mu = \dot{\varepsilon}(x,t) + \dot{\tilde{\varepsilon}}_\mu(y,t)\ \forall \tilde{u}_\mu \in \mathrm{V}\mu \tag{4}$$

The microscale is represented by the RVE and the FEM formulation allows solving the equilibrium problem. The variables and parameters of the RVE are distincts from the material in the macro-continuum and these characteristics are defined for a standard RVE that will be extrapolated to all RVEs in the macroscopic structure. The solution of an RVE (homogenized calculation of displacements, internal forces, stresses and homogenized constitutive tensor) is obtained when the convergence, within the adopted tolerance, of its proposed equilibrium problem is obtained.

Thus, in order to better structure and organize the presentation of the formulation according to a multiscale approach for this work, five steps are considered: Equilibrium equation in the RVE; Hill-Mandel Principle; Homogenization of stresses; Boundary conditions imposed on the RVE; Homogenized Tangent Constituent modulus.

The following expression represents the equilibrium of the solid part of the RVE:

$$\int_{\Omega_\mu^S} \sigma_\mu (y,t) : \nabla^S \eta dV - \int_{\Omega_\mu^S} b(y,t) \times \eta dV - \int_{\partial\Omega_\mu} t^e(y,t) \times \eta dA = 0 \;\; \forall \eta \in \mathrm{V\mu} \tag{5}$$

The Hill and Mandel Principle (Fernandes et al. [4]) says that the macroscale virtual work must equal the of the microscale virtual average volume in the RVE. It establishes that an energetic consistency between the scales and can be given by:

$$\int_{\partial\Omega_\mu} t^e(y,t) \times \dot{\tilde{u}}_\mu dA = 0 \;\; \forall\, \dot{\tilde{u}}_\mu \in \mathrm{V\mu} \tag{6}$$

$$\int_{\Omega_\mu^S} b(y,t) \times \dot{\tilde{u}}_\mu dV = 0 \;\; \forall\, \dot{\tilde{u}}_\mu \in \mathrm{V\mu} \tag{7}$$

The displacement fluctuation field is:

$$\boldsymbol{G_h^{n+1}} = \int_{\Omega_\mu^h} \boldsymbol{B}^T f_y\left(\boldsymbol{\varepsilon^{n+1}} + \boldsymbol{B}\boldsymbol{\tilde{u}_\mu^{n+1}}\right) dV = 0 \tag{8}$$

Where **B** is the global deformation-displacement matrix, Ω_μ^h indicates the discretized domain of the RVE.

The homogenized stress tensor is calculated by Equation (2), considering that the RVE is composed of empty and solid parts, resulting in:

$$\sigma = \sigma(x,t) = \frac{1}{V_\mu}\int_{\Omega_\mu^S} \sigma_\mu(y,t) dV + \frac{1}{V_\mu}\int_{\Omega_\mu^v} \sigma_\mu(y,t) dV \tag{9}$$

The periodic fluctuation condition for the boundary was used in this work. To each side $\boldsymbol{\Gamma_i^+}$do RVE, where the normal direction is $\boldsymbol{n_i^+}$, must match an equal side $\boldsymbol{\Gamma_i^-}$ with normal direction $\boldsymbol{n_i^-}$, being $\boldsymbol{n_i^+} = -\boldsymbol{n_i^-}$. Similarly, for each point y^+set about $\boldsymbol{\Gamma_i^+}$ there must be a point y^- set about $\boldsymbol{\Gamma_i^-}$. So that the displacement fluctuation is periodic in the RVE contour, for each pair (y^+, y^-) of points must have:

$$\tilde{u}_\mu(y^+, t) = \tilde{u}_\mu(y^-, t) \qquad \forall\{y^+, y^-\} \in \partial\Omega_\mu \tag{10}$$

2.2 Cohesive Fracture Model

The adopted cohesive fracture model was developed by Pituba and Souza Neto [10] who described a cohesive law of finite irreversible deformation. The cohesive energy released $\boldsymbol{\phi}$ by the proposed model is given by:

$$\boldsymbol{\phi} = \boldsymbol{\phi}(\delta_n, \delta_s, \boldsymbol{q}) \tag{11}$$

Where δ_n opening the normal mode *I*, δ_s shear mode opening *II* and $\boldsymbol{q}$ is the variable that describes the inelastic processes of cohesion. It is possible to assume that the displacement of the sliding opening is given by a scalar value independent of the direction on the crack surface $\delta_s = |\delta_s|$. For the formulation of cohesive laws in a mixed mode, there is an introduction of an effective opening shift:

$$\delta = \sqrt{\beta^2 \delta_S^2 + \delta_n^2} \tag{12}$$

The β parameter takes values from 0 to 1 according to the values for the normal and shear gaps. Assuming that the energy potential released$\boldsymbol{\phi}$ dependent on δ, the cohesive law is given by:

$$\boldsymbol{t} = \frac{t}{\delta}(\beta^2 \boldsymbol{\delta_S} + \delta_n \boldsymbol{n}) \tag{13}$$

Where $\boldsymbol{n}$ is the normal vector the crack, $\boldsymbol{\delta_s}$ is the shear opening vector located on the crack faces and $\boldsymbol{t}$ is the cohesive stress vector along the crack and *t* is the effective scalar tension given by:

$$t = \sqrt{\beta^{-2}\boldsymbol{t_S}^2 + t_n^2} \tag{14}$$

This relationship shows that β defines the ratio between shear and normal critical tensions. The law of cohesive effective stress for loading case is given by:

$$t = \sigma_c e^{-\delta/\delta_c} \qquad \text{if } \delta = \delta_{max} \text{ and } \dot{\delta} > 0 \tag{15}$$

For the effective scalar stress in the case of discharging to an elastic case, that is, no residual effective aperture displacement is given by:

$$t = \frac{t_{max}}{\delta_{\max}}\delta \qquad \text{se } \delta < \delta_{max} \text{ or } \dot{\delta} \leq 0 \tag{16}$$

Where e is the exponential, σc is the maximum normal cohesive tensile stress, $\dot{\delta}$ is the opening speed, δ_{max} is the maximum effective opening up to the moment of analysis, t_{max} is the maximum effective tension to the moment of analysis and δc represents the critical opening.

If the cracks are closed, a numerical strategy based on Contact Mechanics is adopted. A penalty fact (λ_p) to prevent possible penetration between crack surfaces. This penalty factor is a scalar value parameter given by:

$$t = \lambda_p\delta \qquad \text{se } \lambda_p\delta \leq \sigma_c \tag{17}$$

2.3 Mazars Damage Model

The damage model proposed by Mazars [10] is based on uniaxial tests of concrete specimens based on fundamental hypotheses (Pituba [12]): where locally the damage is due to extensions evidenced by positive signs in at least one of main strain component. The damage is represented by a scalar variable D ($0 \leq D \leq 1$) whose evolution occurs when a reference value for the 'equivalent elongation' is exceeded and the damage is considered isotropic and the damaged concrete behaves as an elastic medium .

The extension state is locally characterized by an equivalent deformation, expressed by (Pituba [12]):

$$\tilde{\varepsilon} = \sqrt{<\varepsilon_1>_+^2 + <\varepsilon_2>_+^2 + <\varepsilon_3>_+^2} \tag{18}$$

Where ε_i is a main strain component, where i = 1, 2 or 3, and$<\varepsilon_i>_+$ is the positive part of you defined by:

$$<\varepsilon_1>_+ = \frac{1}{2}\left[\varepsilon_i + |\varepsilon_i|\right] \tag{19}$$

It was assumed that damage starts when the equivalent deformation reaches a reference deformation value ε_{d0}, determined in uniaxial tensile tests in correspondence to the maximum stress.

Due to the non-symmetry of the concrete response to tension and compression, two independent scalar variables are defined, D_T and D_C, whose values depend on the equivalent deformation and material parameters:

$$D_T(\varepsilon) = 1 - \frac{\varepsilon_{d0}(1-A_T)}{\tilde{\varepsilon}} - \frac{A_T}{\text{e}\ [B_T(\tilde{\varepsilon}-\varepsilon_{d0})]} \tag{20}$$

$$D_C(\varepsilon) = 1 - \frac{\varepsilon_{d0}(1-A_C)}{\tilde{\varepsilon}} - \frac{A_C}{\text{e}\ [B_C(\tilde{\varepsilon}-\varepsilon_{d0})]} \tag{21}$$

Where D_T and D_C are the damage variables for traction and compression respectively, A_T and B_T are characteristic parameters of the material in uniaxial traction, A_C and B_C are material parameters in uniaxial compression and ε_{d0} é the limit elastic deformation. The sub-indexes T and C stand for traction and compression, respectively.

The damage variable is composed of a portion of damage related to traction and another portion corresponding to compression, as suggested by the model. Hence, the damage variable D is given by:

$$D = \alpha_T D_T + \alpha_C D_C \qquad \text{therefore} \quad \alpha_T + \alpha_C = 1 \tag{22}$$

3 Results and Discussions

To verify the feasibility of the proposed formulation, numerical simulations have been performed based on the behaviour of the concrete microstructure. RVEs with dimensions *l*x*l* and thickness *l/10* have been discretized by triangular finite elements. In the transition zone, the contact and cohesive fracture elements have been adopted.

The matrix is considered as damaged elastic according to Mazars criteria. For the elasticity modulus, Mehta and Monteiro [9] say that the value is between 7 and 27 GPa and we adopted 20 GPa. For the Poisson coefficient the value varies between 0.20-0.23 and we adopted 0.20. Also, the values A_T =0.7, B_T =1000, A_C =1.2, B_C =2000 and ε_{d0}=0.0001 have been used for the parameters of the Mazars´model.

The inclusions have been considered as linear elastic with a elasticity modulus equal to 35 GPa, according to Mehta and Monteiro [9], for concretes with medium porosity (20-50 GPa). For the value of the Poisson coefficient, a value equal to 0.35 was considered. In the matrix/aggregate interface region, in cases where fracture have been evaluated, the contact and fracture parameters is: λ_p = 200000, β = 0.707, σ_c = 0.08 MPa. The fracture opening value, δ_c, has been used equal to 0.0568 mm. These values were referenced by Pituba and Souza Neto [9].

For all examples, the RVE presented by Nguyen et al. [12] with random and distinct distribution and inclusion dimensions as shown in Figure 2. This RVE has been chosen because it does not present symmetry between the axes. Its volumetric ratio of aggregates is 35.6%, with 520 triangular finite elements and, when included, 95 fracture elements around the aggregates.

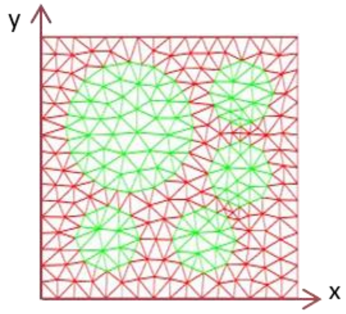

Figure 2. Representative volume element of Nguyen et al. [12].

3.1 Influence of Damage in the Matrix with predominant tension stress on the RVE

First, a tension predominant regime over the RVE is analysed. For this purpose, a macroscopic strain tensor is imposed such as ε_x = 0,00015; ε_y = -0.0000001; γ_{xy} = 0.0000001 subdivide into 30 increments to better capture the dissipative effects and nonlinear behaviour of the material, obtaining the values of the homogenized stresses for the RVE. Figure 3 shows the homogenized stress in the *x* direction with the macroscopic strain on the same axis. Analyses of a RVE with a damaged matrix without fracture elements in the ITZ (RVE 1), a RVE with a non-damaged matrix with fracture elements in the ITZ (RVE 2) and a RVE with a damaged matrix and the presence of fracture elements in the ITZ (RVE 3) has been performed. It is noted that the presence of damage resulted in a loss of stiffness but the fracture is even more impactful on the response.

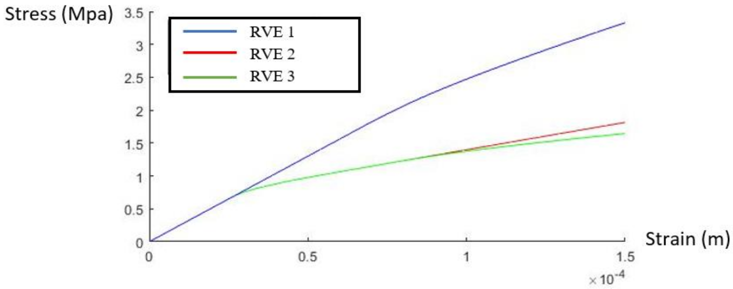

Figure 3. Homogenized normal tensile stress in the *x* direction versus specific macroscopic elongation strain imposed in the *x* direction of the RVE

Figure 4 shows the Stress Colour Chart on the *x* Axis in different situations presented in the previous example (a – RVE 1, b – RVE 2, c – RVE3). In Figure 4-a it is possible to see greater stress effects on inclusions than on the paste. As the inclusions have linear elastic characteristics and do not have fractures, it is expected that they present greater stresses in the aggregates than in the paste, as this matrix presents damage. Figure 4-b shows the Stress Colour Graph on the *x* Axis with the presence of fracture elements. In this case, the stresses in the inclusions are lower. With the presence of these elements, the transmission of tension to the inclusions is smaller and limited. Figure 4-c shows the *x* Axis Stress Colour Graph with the presence of fracture elements and damage to the paste. It is possible to notice that the tension transmission of inclusions and paste remains limited, but the paste presents tension peaks in some elements, thus demonstrating the presence of damage.

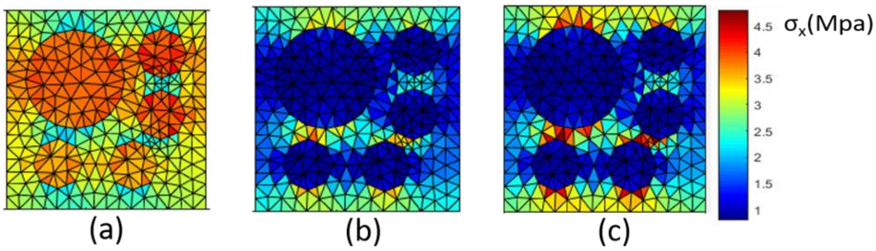

Figure 4. Normal tension distribution in direction *x* inside the RVE: (a) RVE 1, (b) RVE 2, (c) RVE3

3.2 Distribution of Damage in the RVE Mesh

Figure 5 shows the Colour Plot for Damage Variables in each finite element of the RVE. In Figure 5-a, there is no presence of fractures, i. e., RVE1. The region between aggregates exhibits a more intense damage process and also it can been seen the horizontal distribution of a more predominant damage due to tension macrostrain imposed in that direction and, consequently, in the elements located in the vertical direction it presents smaller values. On the other hand, in Figure 5-b, there is the presence of fracture (RVE3) and due to this presence, the transmission of stress is lower between the aggregate and the paste, thus causing damage to the elements in the direction of macroscopic deformation.

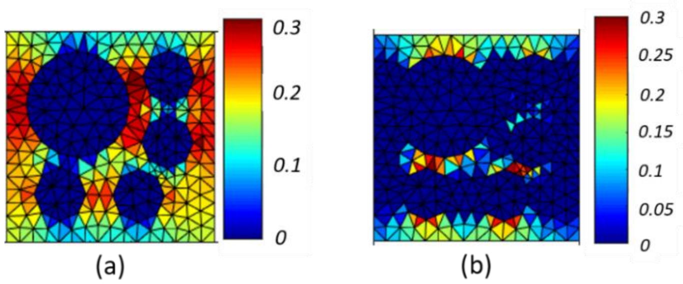

Figure 5. Colour Chart for Variable *D*: a – Without the presence of Fractures (RVE 1), b – With the Presence of Fractures (RVE 3)

3.3 Evolution of the Damage Variable in the RVE

Figure 6 shows the evolution of the damage variable in the RVE for each increment during the analysis. In this example the imposed macroscopic strain applied has been divided into 30 increments. In this evolution, it is possible to notice that the damage arises first in the region located between the inclusions and along the imposed strain it continues to the other elements until a more intense distribution of damage in the RVE.

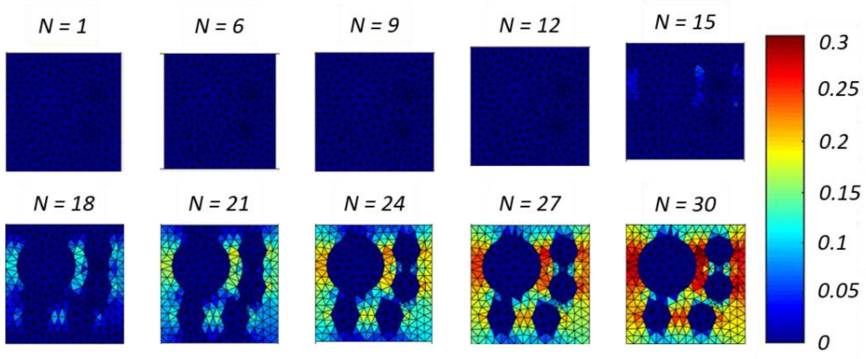

Figure 6. RVE Damage Variable Evolution Color Chart

5 CONCLUSIONS

The proposed modelling aims to simulate the mechanical behaviour of concrete in a multiscale approach capturing the characteristics of damage process in the RVE and its effects on stiffness of the RVE. The analyses present good qualitatively results using simple constitutive models and capturing complex effects on the RVE response. All analyses presented in this work are limited to mesoscale studies.

The finite elements of contact and cohesive fracture included in the Transition Zone present coherent responses already shown by Borges et al. [11]. These elements caused the loss of stiffness in the homogenized response without the total loss of stress transmission between aggregates and cement paste.

The implementation of the Mazars damage model in the cement paste allowed to model the loss of stiffness caused by damage to the material without the need to implement cracks. However, this strategy does not exclude the possibility of crack modelling, and it can combine the two dissipative effects to capture the homogenized response. One of the main contributions of this model is that it can be used to determine the constitutive tensor of the RVE considering each phase, damage and cracking characteristics in the transition zone. This strategy allows combining increasingly complex effects but with the use of simple models.

Acknowledgements. This work was supported by CNPq (National Council for Scientific and Technological Development) [grant numbers 304281/2018-2]; and FAPEG (Goiás Research Foundation) [grant number 201710267000521]; and IFG (Institute Federal of Goiás).

Authorship statement. The authors hereby confirm that they are the sole liable persons responsible for the authorship of this work, and that all material that has been herein included as part of the present paper is either the property (and authorship) of the authors or has the permission of the owners to be included here.

References

[1] J. J. C. Pituba, G. R. Fernandes, "An Anisotropic Damage Model for the Concrete," *Journal of Engineering Mechanics,* vol. 137, pp. 610-624, 2011

[2] G. Z. Voyiadjis, Z. N. Taqieddin, P. I Kattan. "Anisotropic damage–plasticity model for concrete", *International Journal of Plasticity*, vol. 24, pp. 1946– 1965, 2008.

[3] S. M. Giusti, P.J. Blanco; E.A. de Souza Neto; R.A. Feijóo. "An assessment of the Gurson yield criterion by a computational multi-scale approach". *Engineering Computations,* v. 26, n. 3, p. 281-301, 2009.

[4] G. R. Fernandes, J. J. C. Pituba, J. J. C.; E. A. De Souza Neto, "Multi-scale modelling for bending analysis of heteregeneous plates by coupling BEM and FEM". *Engineering Analysis with Boundary Elements*, v. 51; p. 1-13, 2015

[5] J. J. C. Pituba, G. R. Fernandes, J. J. C.; E. A. De Souza Neto, E. A. "Modelling of cohesive fracture and plasticity processes in composite microstructures". *Journal of Engineering Mechanics*, v. 142, pp. 04016069-1 – 04016069-15, 2016.

[6] X. Wang, Z. Yang, A. P. Jivkov, "Monte Carlo simulations of mesoscale fracture of concrete with random aggregates and pores: a size effect study", *Construction and Building Materials,* v. 80, p. 262-272, 2015.

[7] M. Congro, D. Roehl, C. Mejia, "Mesoscale computational modeling of the mechanical behavior of cement composite materials". *Composite Structures*, v. 257, p. 11313, 2021.

[8] J. Mazars, "Application de la mecanique de l'endommagement au comportament nonlineaire et a la rupture Du beton de structure". Thesis, Université Pierre et Marie Curie, Franc, 1984.

[9] P. K. Mehta, P. J. M. Monteiro, P. J. M. Concrete: Microstructure, Properties, and Materials. IBRACON, São Paulo. 2008.

[10] J. J. C. Pituba; E. A. de Souza Neto, E. A. "Modeling of unilateral effect in brittle materials by a mesoscopic scale approach". *Computers and Concrete, An International Journal,* v.15, p. 1-25, 2015.

[11] D. C. Borges, W. M. G. Quaresma, G. R. Fernandes, J. J. C. Pituba. "Evaluation of a proposed model for concrete at mesoscopic scale". *IBRACON Structures and Materiais Journal,* v. 10, n. 5, p. 1087-1112, 2017.

[12] J. J. C. Pituba. "Estudo e Aplicação de Modelos Constitutivos para o Concreto Fundamentos na Mecânica do Dano Contínuo". Dissertação, Universidade de São Paulo, Brasil, 1998.

[13] V. P. Nguyen; O. Lloberas Valls; M. Stroeven; L. J. Sluys. "On the existence of representative volumes for softening quasi-brittle materials – a failure zone averaging scheme", *Computer Methods in Applied Mechanics Engineering*, v. 199, 2010.